Tohoku J. Exp. Med., 2023, **261**, 239-247

# Development of a Novel and Simple Anti-Metastatic Cancer Treatment Targeting Vasohibin-2

**Eun-Seo Lee,[1] Yasuhiro Suzuki,[1,2] Hideki Tomioka,[3] Hironori Nakagami[4] and Yasufumi Sato[1,2]**

[1]Department of Vascular Biology, Institute of Development, Aging and Cancer, Tohoku University, Sendai, Miyagi, Japan
[2]New Industry Creation Hatchery Center, Tohoku University, Sendai, Miyagi, Japan
[3]Funpep Company Limited, Ibaraki, Osaka, Japan
[4]Department of Health Development and Medicine, Osaka University Graduate School of Medicine, Suita, Osaka, Japan

Vasohibin-2 (VASH2), a homologue of vasohibin-1 (VASH1), is overexpressed in various cancer cells and promotes tumor progression. We therefore regard VASH2 as a molecular target for cancer treatment. Here we applied vaccine technology to develop a therapy against VASH2. We selected two amino acid sequences of VASH2 protein; the MTG and RRR peptides, which contain possible B cell epitopes. These sequences are identical between the human and murine VASH2 proteins and distinct from those of the VASH1 protein. We conjugated these peptides with the carrier protein keyhole limpet hemocyanin, mixed with an adjuvant, and injected subcutaneously twice at a 2-week interval in mice. Both vaccines increased antibodies against the antigen peptide; however, only the MTG peptide vaccine increased antibodies that recognized the recombinant VASH2 protein. When Lewis lung cancer (LLC) cells were subcutaneously inoculated, tumors isolated from mice immunized with the MTG peptide vaccine showed a significant decrease in the expression of epithelial-to-mesenchymal transition (EMT) markers. EMT is responsible for cancer cell invasion and metastasis. When the LLC cells were injected into the tail vein, the MTG peptide vaccine inhibited lung metastasis. Moreover, the MTG peptide vaccine inhibited the metastasis of pancreatic cancer cells to the liver in an orthotopic mouse model, and there was a significant inverse correlation between the ELISA titer and metastasis inhibition. Therefore, we propose that the MTG peptide vaccine is a novel anti-metastatic cancer treatment that targets VASH2 and can be applied even in the most malignant and highly metastatic pancreatic cancer.

**Keywords:** cancer metastasis; epithelial-to-mesenchymal transition; peptide vaccine; vasohibin-2
Tohoku J. Exp. Med., 2023 November, **261** (3), 239-247.
doi: 10.1620/tjem.2023.J076

## Introduction

Vasohibin-1 (VASH1) is an endothelium-derived angiogenesis inhibitor (Watanabe et al. 2004), and vasohibin-2 (VASH2) is a homologue of VASH1 (Shibuya et al. 2006). The overall homology between human VASH1 and VASH2 is 52.5% considering the amino-acid sequence (Shibuya et al. 2006). Recent genomic studies revealed that both *VASH1* and *VASH2* are highly conserved among species. Lower organisms possess a single ancestral *VASH*, and this ancestral *VASH* has evolved into *VASH1* and *VASH2* in vertebrates; VASH2 is closer to the ancestral VASH (Sato 2013). Although VASH1 is mainly expressed in endothelial cells, VASH2 is not expressed in normal tissues after birth, except in the testes, but its expression is augmented under pathological conditions, including cancer (Sato 2013). Small vasohibin-binding protein (SVBP) has been isolated as a binding partner of VASHs (Suzuki et al. 2010). Because VASHs lack classical signal sequences for secretion, it is unclear whether they are secreted. Isolation of SVBP verified that VASHs are secretory proteins and that SVBP acts as a secretory chaperone of VASHs (Suzuki

Received July 6, 2023; revised and accepted September 2, 2023; J-STAGE Advance online publication September 14, 2023
Correspondence: Yasufumi Sato, Department of Vascular Biology, Institute of Development, Aging and Cancer, Tohoku University, 4-1 Seiryo-machi, Aoba-ku, Sendai, Miyagi 980-8575, Japan.
e-mail: yasufumi.sato.b3@tohoku.ac.jp

et al. 2010).

VASH2 overexpression has been observed in various cancers. Overexpression of VASH2 acts on both cancer cells and cancer microenvironment cells because VASH2 stimulates tumor angiogenesis (Takahashi et al. 2012; Xue et al. 2013; Kitahara et al. 2014), activates cancer-associated fibroblasts (Suzuki et al. 2017), and induces epithelial-to-mesenchymal transition (EMT) in cancer cells (Norita et al. 2017; Tu et al. 2017; Zhang et al. 2018). Accordingly, overexpression of VASH2 is responsible for cancer progression, and the abrogation of VASH2 expression or its activity exhibits apparent antitumor effects (Takahashi et al. 2012; Xue et al. 2013; Koyanagi et al. 2013; Iida-Norita et al. 2019). Therefore, we proposed VASH2 as a potential molecular target for cancer treatment.

Vaccines are simple, well-established, cost-effective, and long-term treatments that protect against various diseases. Recent developments in cancer vaccines have attracted considerable research interest. In general, cancer vaccines stimulate and activate cytotoxic T cells to reject cancer cells; this strategy has been promoted by the discovery of various tumor-specific antigens (Parmiani et al. 2014). However, the objective clinical response rates of cancer vaccines remain low, and several efforts to improve their efficacy are underway (Saxena et al. 2021; Morse et al. 2021).

Here, we attempted to develop a feasible antibody-based drug targeting VASH2 using a peptide vaccine technique (Nakagami et al. 2014). We selected a partial peptide of VASH2 and induced B cell-mediated immune responses to produce blocking antibodies targeting VASH2.

## Materials and Methods

*Preparation of the VASH2 peptide vaccine*

Two partial amino acid sequences of VASH2, MTGSAADTHR (MTG) and RRRQASPPRR (RRR), were selected (Fig. 1), which contained possible B cell epitopes based on a high antigenicity analysis of the predicted three-dimensional structure and epitope information (Jespersen et al. 2017). The peptides and keyhole-limpet hemocyanin (KLH) of the carrier protein were conjugated using glutaraldehyde as a condensing agent as previously described (Yoshida et al. 2020).

*Vaccination*

All animal experiments were performed in accordance with the protocol approved by the Committee on Animal Experimentation of Tohoku University. Wild-type male C57BL/6J mice (8 weeks old) were obtained from Charles River Laboratories Japan (Yokohama, Japan) and used for vaccination, as previously described (Yoshida et al. 2020). Briefly, various doses of the peptide vaccines were mixed with equal volumes of Freund's adjuvant (Wako Pure Chemical Industries, Tokyo, Japan) or Alhydrogel adjuvant (San Diego, CA, USA) before injection and emulsification. One hundred microliters of the peptide vaccine mixture was intradermally injected into each mouse. The antigen dose corresponded to the peptide dose in the conjugated KLH peptide. The vaccination protocol consisted of two injections at 2-week intervals. The primary injection was performed with complete Freund's adjuvant, and the secondary injection was

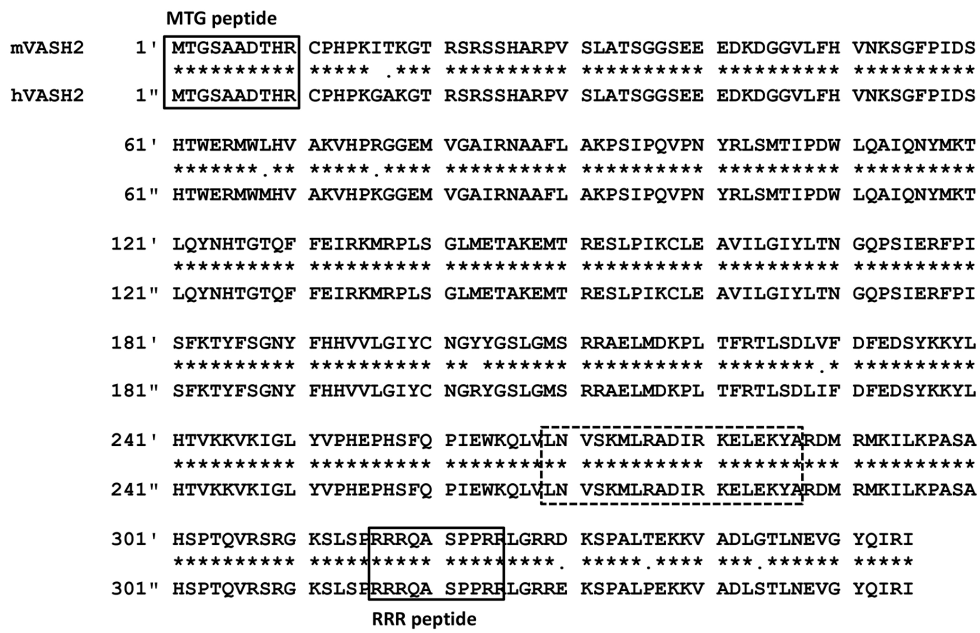


Fig. 1. Amino acid sequences of the vasohibin-2 (VASH2) peptides for the vaccine.
Amino acid sequences of human (h) VASH2 and murine (m) VASH2 are shown. The stars indicate identical amino acids. Solid boxes indicate the peptides used for the vaccine, MTG and RRR peptides. The dashed box indicates the peptide of the previous monoclonal antibody used to inhibit angiogenesis.

performed with incomplete Freund's adjuvant. We also injected mice with an emulsion of KLH with adjuvant as the negative control. Blood samples were collected from the facial vein and subjected to an enzyme-linked immunosorbent assay (ELISA).

*ELISA*

The peptides were conjugated to bovine serum albumin at the Peptide Institute Inc. (Osaka, Japan). Recombinant human VASH2 protein has been previously described (Shibuya et al. 2006). Serum antibody titers were measured using conjugates as previously described (Yoshida et al. 2020). Briefly, a peptide-bovine serum albumin conjugate or recombinant VASH2 protein was dissolved in carbonate buffer (10 μg/mL or 1 μg/mL) and coated onto a 96 well immuno-plate (MaxiSorp, Nunc). The coated plates were incubated overnight at 4°C. After blocking with a 5% skim milk solution, the samples were serial diluted from 20- to 62,500-fold with a 5% skim milk solution, and were incubated in the plate overnight at 4°C. The plates were then washed with phosphate buffered saline, and a mouse IgG horseradish peroxidase (HRP)-conjugated antibody was added. The plates were incubated for 3 h at room temperature and then washed. The antigen-antibody reaction was detected using 3,3′,5,5′-tetramethylbenzidine solution and 0.5 N sulfuric acid. Finally, the absorbance at 450 nm was measured with an iMark Microplate Reader (Bio-Rad, Hercules, CA, USA).

*Cell cultures*

The culture of Lewis lung cancer (LLC) cells has been previously described (Hosaka et al. 2009). In addition, we generated the murine pancreatic cancer cell line by the use of *LSL-KRas*$^{G12D/+}$*;LSL-Trp53*$^{R172H/+}$*;Pdx-1-Cre* (*KPC*) mice, a model of pancreatic ductal adenocarcinoma (Iida-Norita et al. 2019). Since the KPC mice had a mixed genetic background of C57BL/6 and 129, we backcrossed more than 10 times and generated KPC mice on a C57BL/6 genetic background. We then isolated pancreatic cancer cells (KPC$^{C57}$ cells) from the pancreatic cancer tissue and maintained them in Dulbecco's modified Eagle's medium supplemented with 10% fetal bovine serum. KPC$^{C57}$ cells were transfected with pGL4.51 [luc2/CMV/Neo] vector (Promega, Madison, WI, USA) using FuGENE HD transfection reagent (Promega) according to the manufacturer's instructions. Transfected cells were selected in a culture medium supplemented with G418 (FUJIFILM Wako Pure Chemical Corporation, Tokyo, Japan) for 3 weeks. The selected G418-resistant cells were seeded into 96-well plates at 0.5 cell/well to form single cell colonies. Bioluminescence was used to select clones with luciferase activity using an *in vivo* imaging system (IVIS Lumina II; Xenogen, Alameda, CA, USA). The clones stably expressing firefly luciferase under the control of the cytomegalovirus promoter were designated as KPC$^{C57Luc}$.

*Quantitative reverse transcription-polymerase chain reaction (RT-PCR)*

Fourteen days after the second vaccination, $1.0 \times 10^7$ LLC cells were subcutaneously inoculated. Tumors were recovered 2 weeks after inoculation, and total RNA was extracted using QIAzol Lysis Reagent (QIAGEN, Hilden, Germany) and purified using the RNeasy Mini Kit (QIAGEN). First-strand cDNA was synthesized by reverse transcription using ReverTra Ace (TOYOBO, Osaka, Japan). Quantitative RT-PCR was performed using a CFX96 real-time RT-PCR detection system (Bio-Rad Laboratories) according to the manufacturer's instructions. The thermal cycling conditions consisted of an initial denaturation at 95°C for 3 min, followed by 40 cycles of 10 s at 95°C, 10 s at 56°C and 30 s at 72°C. Relative mRNA levels of target genes were normalized to the level of beta-actin mRNA. The primer pairs used were as follows: mCD31 forward 5′-TTCAGCGAGATCCTGAGGGTC-3′ and reverse 5′-CGCTTGGGTGTCATTCACGAC-3'; m*Twist1* forward 5′-GCCAGGTACATCGACTTCCT-3′, and reverse 5′-CCAGACGGAGAAGGCGTAG-3'; mSnai forward 5′-GAGGACAGTGGCAAAAGCTC-3′ and reverse 5′-CAGCTGCTTGGGAAGTTGG-3'; mZeb1 forward 5′-CTCCCAGTCAGCCACCTTTA-3′ and reverse 5′-GGTTCACAGAATCGGCGATC-3'.

*Metastasis models*

Eight-week-old male C57BL/6J mice (Charles River Laboratories Japan) were used in this study. All animal experiments were approved by the Tohoku University Center for Gene Research and were carried out according to the guidelines for animal experimentation at Tohoku University.

An experimental metastasis model was established as previously described (Ito et al. 2013). Briefly, $5 \times 10^5$ LLC cells were injected into the tail vein of mice. Sixteen days after the injection, the mice were euthanized, and their lungs were obtained. Lungs were extracted, incubated overnight with 4% paraformaldehyde, dehydrated in graded ethanol and xylene, and embedded in paraffin wax. Vertical sections (5 $\mu$m) of the entire lung were prepared for conventional hematoxylin and eosin staining.

An orthotopic pancreatic cancer model was constructed as follows: KPC$^{C57Luc}$ cells were suspended in ice-cold serum free Dulbecco's modified Eagle's medium and mixed gently with the same volume of ice-cold Matrigel (Corning Life Sciences, Corning, NY, USA) to prepare a homogenous suspension. We anesthetized 6-week-old female C57BL/6 mice, opened their abdominal cavities, and carefully exteriorized the pancreatic tail attached to the spleen. We then injected 50 $\mu$L of the cell suspension containing $2.5 \times 10^5$ KPC$^{C57Luc}$ cells to the pancreatic tail using a 27 gauge-needle. The pancreas and spleen were returned to the peritoneal cavity and the incision was closed with surgical sutures. On day 1 and day 15, we immunized the mice with the MTG peptide vaccine. Thirty-five days after

inoculation, we evaluated the effects of the vaccination. To evaluate the primary tumor growth, we performed *in vivo* bioluminescence imaging using an IVIS system. To evaluate metastasis, livers were excised and subjected to *ex vivo* bioluminescence detection using the IVIS system. Bioluminescent signal activity was quantified using Living Image software (Xenogen).

*Immunohistochemical analysis*

Immunohistochemical analysis was performed as described previously (Suzuki et al. 2017). Briefly, primary tumors were obtained, fixed overnight with 4% paraformaldehyde, dehydrated in graded ethanol and xylene, and embedded in paraffin wax. Thereafter, tissue sections (5 $\mu$m) were autoclaved in citrate buffer (pH 6.0) for 5 min for antigen retrieval prior to incubation with the primary antibody. The antibody against CD31 (Cell Signaling Technology, Beverly, MA, USA) was used as the primary antibody, and the antibody conjugated with Alexa Fluor 488 (Thermo Fisher Scientific, Waltham, MA, USA) was used as the secondary antibody. Nuclei were then counterstained using DAPI (Thermo Fisher Scientific). Tissue autofluorescence was eliminated using the TrueVIEW autofluorescence quenching kit (Vector Laboratories, Peterborough, UK). Microphotographs and fluorescence images were captured using a KEYENCE BZ-9000 microscope system (Keyence Corporation, Osaka, Japan).

*Statistical analysis*

Data are expressed as the mean ± standard deviation (SD), where indicated. Wilcoxon rank sum test or Spearman's rank correlation coefficient were used to test for significant differences. Statistical significance was set at $P < 0.05$.

## Results

*Development of VASH2 peptide vaccine*

To develop a peptide vaccine that could target VASH2, we applied the BepiPred tool for the prediction of B cell epitope and selected 2 amino acid sequences of VASH2, the MTG and RRR peptides, having the highest scores (Jespersen et al. 2017). Importantly, these amino acid sequences were identical between human and mouse VASH2 proteins (Fig. 1) and distinct from those of the VASH1 protein (Supplementary Fig. S1). The vaccination protocol consisted of two injections of peptide vaccines (5 $\mu$g or 20 $\mu$g) at 2-week intervals. To obtain an adequate immune response, peptides were conjugated to KLH and mixed with an adjuvant. We collected blood samples on day 28 and analyzed the ELISA titers against each antigen peptide and recombinant VASH2 protein. Mice immunized with each peptide vaccine showed a significant increase in ELISA titers against MTG and RRR peptides (Fig. 2A, B). Instead, the ELISA titer of the recombinant VASH2 protein was significantly higher in mice immunized with the MTG peptide vaccine than in those immunized with the RRR peptide vaccine (Fig. 2C, D). These results indicated that the MTG peptide vaccine was able to induce antibodies that recognized not only antigen peptides but also whole VASH2 proteins.

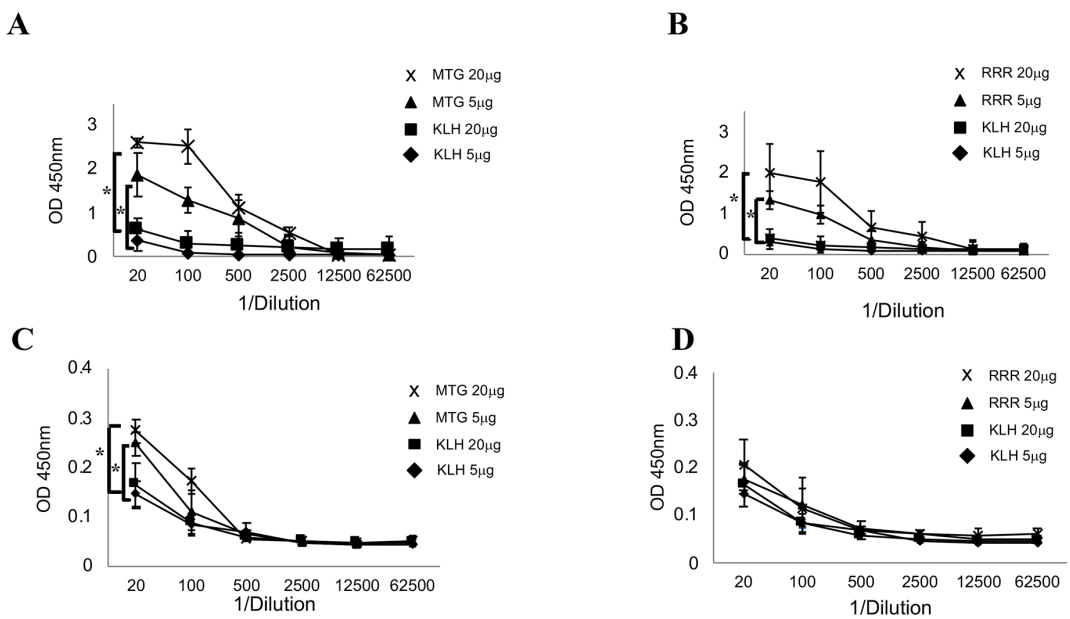


Fig. 2. Enzyme-linked immunosorbent assay (ELISA) titers of the collected serum samples.
The collected serum samples were analyzed using ELISA. (A) ELISA titers against MTG peptides (N = 5, each). (B) ELISA titers against RRR peptides (N = 5, each). (C) ELISA titers against recombinant vasohibin-2 (VASH2) protein (N = 5, each). (D) ELISA titers against recombinant VASH2 protein (N = 5, each). The titers are expressed as the dilution of serum, and data are represented as mean ± SD. *$P < 0.05$ vs. control KLH.

*Inhibition of EMT in cancer cells by the vaccine*

To investigate the possible effects of peptide vaccines on tumors, we examined tumor growth in mice. Following vaccination, we subcutaneously inoculated the LLC cells. Two weeks after inoculation, the mice were euthanized, blood samples were collected, and tumor tissues were evaluated. Because VASH2 is known to stimulate tumor growth by inducing tumor angiogenesis, we examined *mCD31* mRNA expression in tumors as a marker of angiogenesis. The *mCD31* mRNA expression was slightly suppressed in the high-dose MTG peptide vaccine group, although the difference was not statistically significant (Fig. 3A). In addition to angiogenesis, VASH2 stimulates EMT in cancer cells, which causes tumor progression. Accordingly, the mRNA levels of the EMT markers, m*Twist1*, m*Snail*, and m*Zeb1*, were significantly suppressed by the MTG peptide vaccine (Fig. 3B). EMT is involved in cancer cell migration, invasion, and metastasis (Marcucci et al. 2016). Therefore, we tested whether the antisera obtained from the high-dose MTG peptide vaccine group affected cancer cell migration. As shown in Fig. 3C, antisera from the high-dose MTG peptide vaccine group significantly inhibited the migration of LLC cells in culture. Antisera also inhibited the migration of human rhabdomyosarcoma RH30 cells (data not shown).

*Inhibition of cancer metastasis by the vaccine*

To test whether the MTG peptide vaccine could prevent cancer metastasis, we used a murine experimental metastasis model. Following the vaccination of mice with the MTG peptide, LLC cells were injected into the tail vein. The mice were euthanized 3 weeks after LLC injection and lung metastasis was analyzed. Vaccination with the MTG peptide, especially at a high dose (20 $\mu$g), inhibited lung metastasis of LLC cells, and this inhibition was evident when the ELISA titer against the whole VASH2 protein was

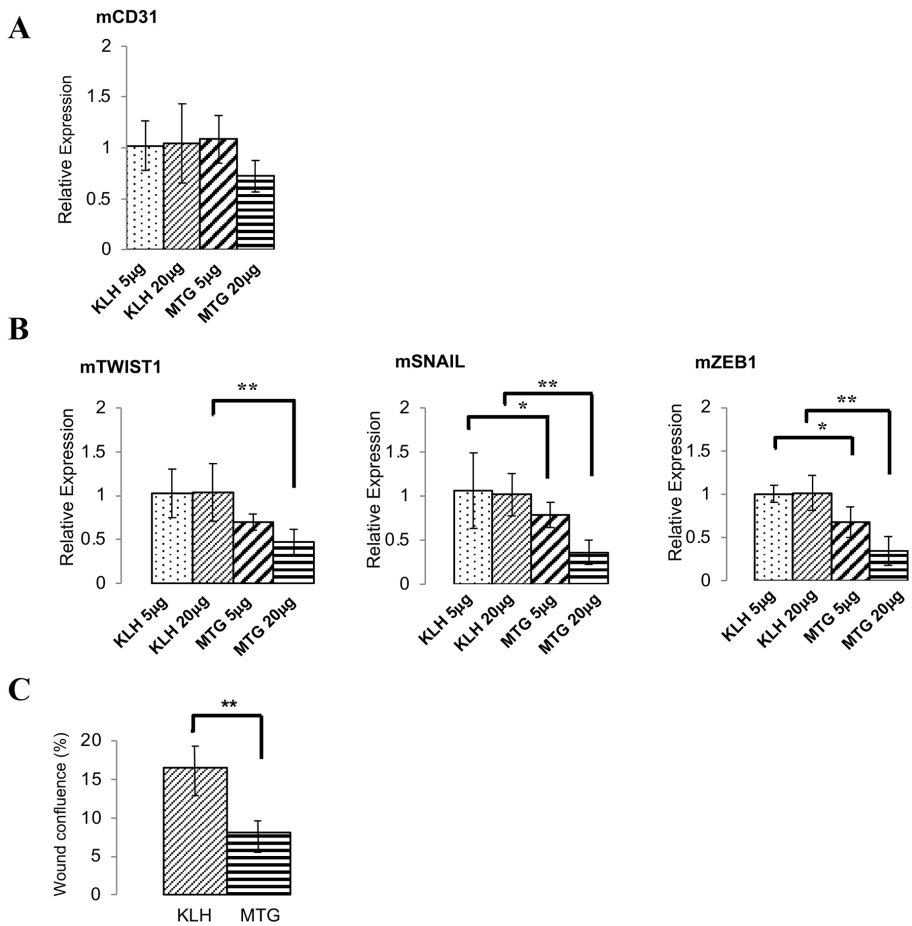


Fig. 3. Effect of MTG peptide vaccine on the mice subcutaneously inoculated with Lewis lung cancer (LLC) cells.
Following MTG peptide vaccination, LLC cells were inoculated subcutaneously into the mice. Two weeks after inoculation, tumor tissues and blood samples were obtained. (A) Expression of *mCD31* mRNA in tumor tissues was quantified and compared (N = 3, each). (B) The expression levels of m*Twist1*, m*Snail*, and m*Zeb1* mRNA in tumor tissues were quantified and compared (N = 3, each). (C) The wound migration of cultured LLC cells was tested. Antisera (1%) from the 20 $\mu$g MTG peptide vaccine group were added to the culture during the wound migration (N = 3). The percentage of wound healing was calculated using the formula $W^{\%} = \{(W^0 - W^t)/W^0\} \times 100$, where $W^{\%}$ is the percentage of wound healing, $W^0$ is the area of wound at time 0, and $W^t$ is the area of wound after different times of healing. All quantitative data are shown as mean ± SD. $^*P < 0.05$ and $^{**}P < 0.01$ vs. control KLH.

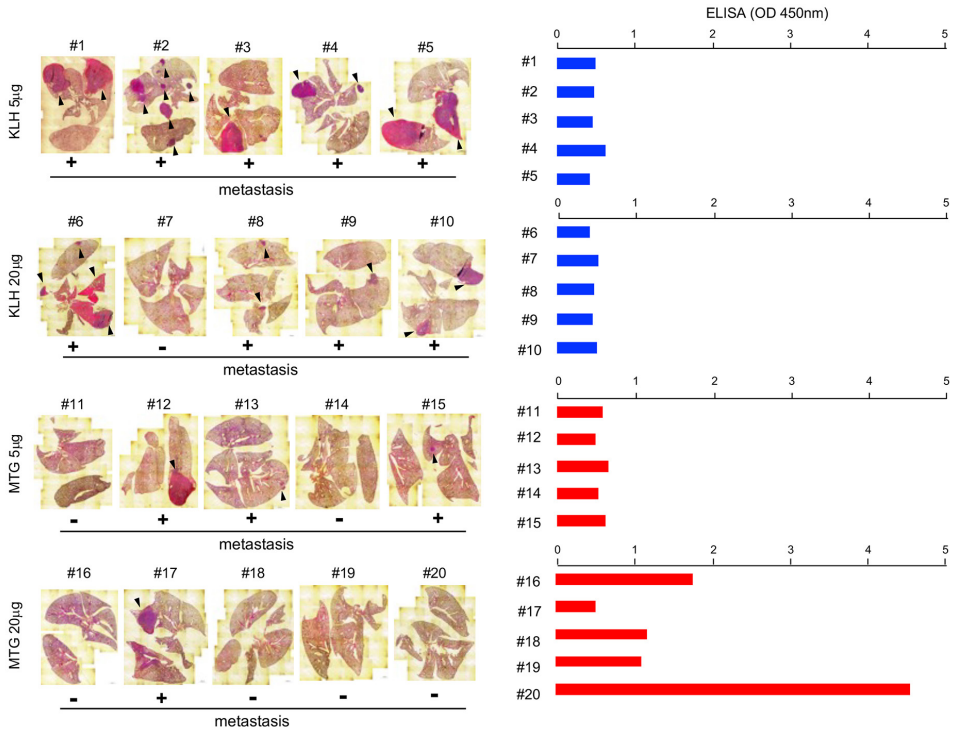


Fig. 4. Effect of the MTG peptide vaccine in the experimental metastasis model.
Following MTG peptide vaccination, Lewis lung cancer (LLC) cells were injected into the tail veins of mice. Three weeks after tail vein injection, lung metastasis was analyzed. Representative images of hematoxylin and eosin-stained lungs are shown on the left. Triangles indicate metastasis. ELISA titers against the MTG peptide are shown on the right.

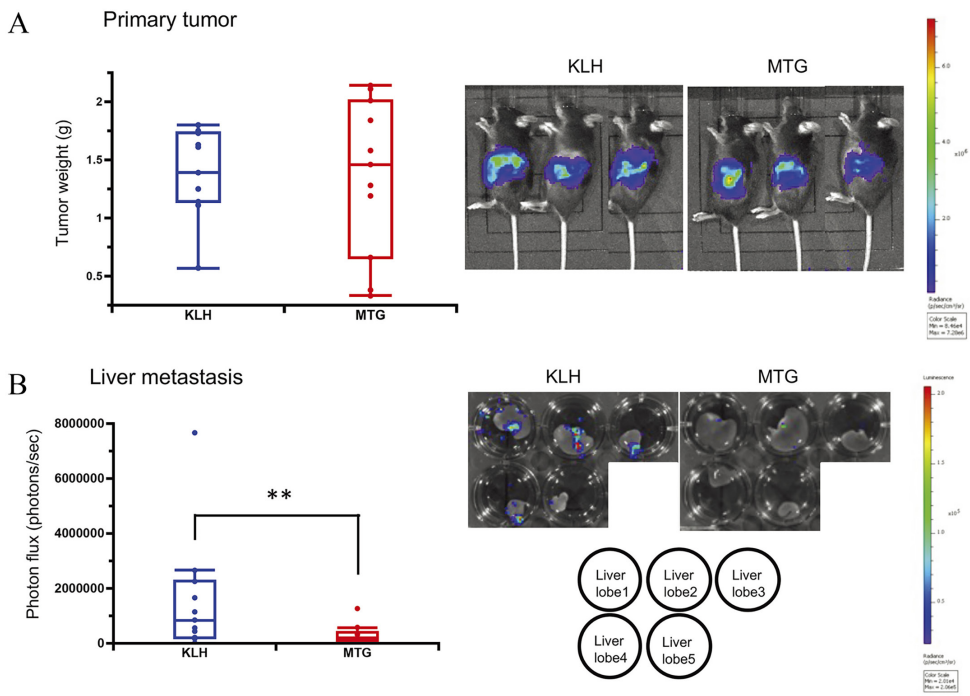


Fig. 5. Effect of the MTG peptide vaccine in the spontaneous metastasis model.
Following the orthotopic inoculation of KPC$^{C57Luc}$ cells in mice, MTG peptide vaccination was initiated the next day. Thirty-five days after inoculation, the primary tumors and liver metastases were analyzed and compared. (A) Primary tumors were observed using *in vivo* bioluminescence imaging (N = 13, each). Representative images are shown on the right. (B) Livers were excised and subjected to *ex vivo* bioluminescence imaging (N = 13, each). Representative images are shown on the right. All quantitative data are shown as a Box and Whisker Plot. $^{**}P < 0.01$ vs. control KLH.

high (Fig. 4).

To further confirm the antimetastatic effect of the MTG peptide vaccine, we examined spontaneous cancer metastasis using an orthotopic pancreatic cancer model. We orthotopically inoculated KPC$^{C57Luc}$ cells into mice and started the MTG peptide vaccination the next day with 2 weeks interval. Thirty-five days after the inoculation, the effects of the MTG peptide vaccine were examined. *In vivo* imaging revealed that primary tumor growth was not affected by the vaccination (Fig. 5A). We then euthanized the mice and examined tumor metastasis. The liver is the most common organ for metastasis in pancreatic cancer. We found that the metastasis of KPC$^{C57Luc}$ cells to the liver was significantly prevented by the MTG peptide vaccine (Fig. 5B). Moreover, we observed a significant inverse correlation between the ELISA titer and liver metastasis (Fig. 6). We further examined tumor vessels in the primary tumor, and found that the MTG peptide vaccine did not significantly inhibited tumor angiogenesis (Fig. 7).

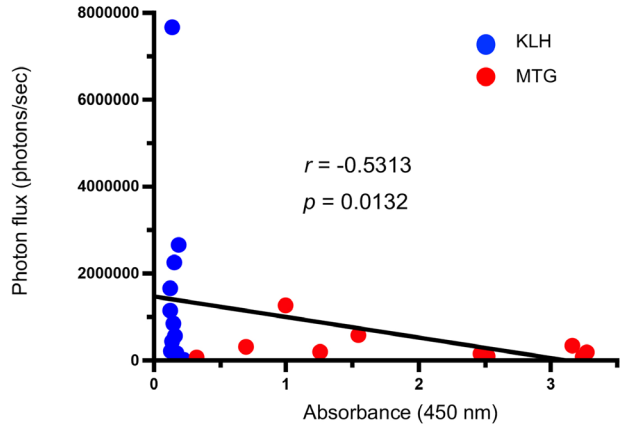


Fig. 6. Inverse correlation of the enzyme-linked immunosorbent assay (ELISA) titer and liver metastasis in the spontaneous metastasis model.
The correlation between ELISA titers and *ex vivo* bioluminescence data of KLH (N = 11) and MTG peptide vaccine (N = 10) are shown.

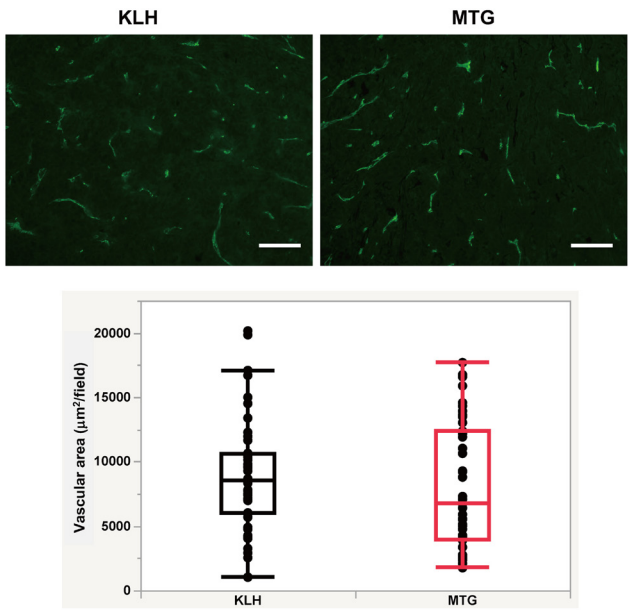


Fig. 7. Effect of the MTG peptide vaccine on tumor angiogenesis.
Primary tumors of the orthotopic mouse model of pancreatic cancer were analyzed for tumor angiogenesis. The sections were immunostained with CD31 to detect tumor vessels. CD31 positive vascular area ($\mu m^2$/field) was measured to quantify tumor angiogenesis. All quantitative data are shown as a Box and Whisker Plot. There was no significant difference in the area of tumor vessels in mice treated with KLH (N = 11) and MTG peptide vaccine (N = 10). Bar = 100 $\mu$m.

## Discussion

Cancer/testis antigens (CTAs) are a large family of antigens that are expressed in tumors, but not in normal tissues, except for the testis (Salmaninejad et al. 2016). Because of this tumor-restricted pattern of expression, CTAs are recognized as ideal targets of cancer vaccines, and cancer vaccines help stimulate and activate cytotoxic T cells to reject cancer cells. VASH2 is considered a member of the CTA family; however, it is a functional and secretory protein that stimulates cancer cells as well as tumor microenvironment cells for cancer progression. Therefore, we do not believe that VASH2 is an ideal target for T cell-mediated cytotoxicity.

Here, we attempted to induce a B cell-mediated immune response to produce antibodies that block the effects of VASH2. To produce antibodies efficiently, we selected two partial amino acid sequences of VASH2 that contained possible B cell epitopes, conjugated them with KLH, and subcutaneously injected them with adjuvants. Although these two peptide vaccines, namely the MTG and RRR peptide vaccines, sufficiently induced antibodies against their antigen peptides, the MTG peptide vaccine induced antibodies that could recognize the recombinant VASH2 protein, whereas the RRR peptide vaccine could not. The reason for this difference is probably that the MTG peptide is located on the outer surface of the three-dimensional structure of the VASH2 protein, whereas the RRR peptide is not. Therefore, we selected the MTG peptide vaccine for further evaluation.

We previously developed an anti-VASH2 monoclonal antibody that blocks the pro-angiogenic activity of VASH2 (Koyanagi et al. 2017). Therefore, we considered VASH1 as a possible functional domain that regulates angiogenesis. We assumed the presence of a similar region in the VASH2 protein, created a synthetic peptide of the corresponding domain (Fig. 1, dashed box), and raised monoclonal antibodies against that peptide. Among the several clones, we selected the one that showed blocking activity against VASH2-mediated angiogenesis. The manner in which the peptides were selected differed in the present study. Because we utilized vaccination technology, we searched for amino acid sequences of VASH2 that contained a possi-

ble B cell epitope and obtained an MTG peptide vaccine that induced antibodies recognizing recombinant VASH2 protein. The MTG peptide vaccine reduced the expression of EMT markers more efficiently than did the angiogenesis markers in cancer tissues. Therefore, the responsible domains in VASH2 for EMT induction in cancer cells and angiogenic stimulation in endothelial cells may differ. A more detailed analysis of the structure-function relationship of the VASH2 protein is required in the future.

EMT is associated with tumor invasion and metastasis (Marcucci et al. 2016), and VASH2 has been shown to play a critical role in the regulation of EMT in various cancer models (Xue et al. 2014; Norita et al. 2017; Tu et al. 2017; Zhang et al. 2018). Therefore, we tested the possible anti-metastatic effects of the MTG peptide vaccine in mice. Accordingly, we demonstrated that the MTG peptide vaccine inhibited cancer metastasis when the ELISA titer was high. These observations indicate that the MTG peptide vaccine raises antibodies that can recognize the entire VASH2 protein, and when the titer is sufficiently high, the antibodies inhibit cancer metastasis by blocking the action of VASH2 on cancer cell EMT. As many patients with cancer die because of metastasis, our results should have a considerable effect.

Pancreatic cancer is a highly metastatic malignancy. Anti-angiogenic treatments are ineffective, and novel therapeutic targets are anticipated for the effective treatment of pancreatic cancer (Hosein et al 2020; Ricci et al. 2022). The involvement of VASH2 in the progression of pancreatic cancer has been demonstrated, as knockdown of vash2 in KPC-derived pancreatic cancer cells or genetic deletion of *Vash2* in KPC mice significantly reduces metastasis (Iida-Norita et al. 2019). Here, we employed an orthotic pancreatic cancer model as a spontaneous metastasis model and examined the effects of an MTG peptide vaccine. The MTG peptide vaccine inhibited the metastasis of pancreatic cancer cells to the liver, and there was a significant inverse correlation between the ELISA titer and metastasis inhibition. Therefore, we expect that if sufficient titers are maintained, patients immunized with the MTG peptide vaccine would be resistant to metastasis, even in the most malignant pancreatic cancer.

In conclusion, we established an MTG peptide vaccine that recognizes the recombinant VASH2 protein and confirmed its antimetastatic activity in a mouse model. Therefore, we propose that the MTG peptide vaccine is a novel option for cancer treatment by targeting VASH2.

## Acknowledgments

This work was supported by the grant numbered 21cm0106201h0006 from the Japan Agency for Medical Research and Development to Y.S. We thank Ms. Yuriko Fujinoya for her technical assistance.

## Conflict of Interest

The authors declare no conflict of interest.

## References

Hosaka, T., Kimura, H., Heishi, T., Suzuki, Y., Miyashita, H., Ohta, H., Sonoda, H., Moriya, T., Suzuki, S., Kondo, T. & Sato, Y. (2009) Vasohibin-1 expression in endothelium of tumor blood vessels regulates angiogenesis. *Am. J. Pathol.*, **175**, 430-439.

Hosein, A.N., Brekken, R.A. & Maitra, A. (2020) Pancreatic cancer stroma: an update on therapeutic targeting strategies. *Nat. Rev. Gastroenterol. Hepatol.*, **17**, 487-505.

Iida-Norita, R., Kawamura, M., Suzuki, Y., Hamada, S., Masamune, A., Furukawa, T. & Sato, Y. (2019) Vasohibin-2 plays an essential role in metastasis of pancreatic ductal adenocarcinoma. *Cancer Sci.*, **110**, 2296-2308.

Ito, S., Miyashita, H., Suzuki, Y., Kobayashi, M., Satomi, S. & Sato, Y. (2013) Enhanced cancer metastasis in mice deficient in vasohibin-1 gene. *PLoS One*, **8**, e73931.

Jespersen, M.C., Peters, B., Nielsen, M. & Marcatili, P. (2017) BepiPred-2.0: improving sequence-based B-cell epitope prediction using conformational epitopes. *Nucleic Acids Res.*, **45**, W24-W29.

Kitahara, S., Suzuki, Y., Morishima, M., Yoshii, A., Kikuta, S., Shimizu, K., Morikawa, S., Sato, Y. & Ezaki, T. (2014) Vasohibin-2 modulates tumor onset in the gastrointestinal tract by normalizing tumor angiogenesis. *Mol. Cancer*, **13**, 99.

Koyanagi, T., Suzuki, Y., Komori, K., Saga, Y., Matsubara, S., Fujiwara, H. & Sato, Y. (2017) Targeting human vasohibin-2 by a neutralizing monoclonal antibody for anti-cancer treatment. *Cancer Sci.*, **108**, 512-519.

Koyanagi, T., Suzuki, Y., Saga, Y., Machida, S., Takei, Y., Fujiwara, H., Suzuki, M. & Sato, Y. (2013) In vivo delivery of siRNA targeting vasohibin-2 decreases tumor angiogenesis and suppresses tumor growth in ovarian cancer. *Cancer Sci.*, **104**, 1705-1710.

Marcucci, F., Stassi, G. & De Maria, R. (2016) Epithelial-mesenchymal transition: a new target in anticancer drug discovery. *Nat. Rev. Drug Discov.*, **15**, 311-325.

Morse, M.A., Gwin, W.R.3rd & Mitchell, D.A. (2021) Vaccine therapies for cancer: then and now. *Target. Oncol.*, **16**, 121-152.

Nakagami, H., Koriyama, H. & Morishita, R. (2014) Peptide vaccines for hypertension and diabetes mellitus. *Vaccines* (*Basel*), **2**, 832-840.

Norita, R., Suzuki, Y., Furutani, Y., Takahashi, K., Yoshimatsu, Y., Podyma-Inoue, K.A., Watabe, T. & Sato, Y. (2017) Vasohibin-2 is required for epithelial-mesenchymal transition of ovarian cancer cells by modulating transforming growth factor-$\beta$ signaling. *Cancer Sci.*, **108**, 419-426.

Parmiani, G., Russo, V., Maccalli, C., Parolini, D., Rizzo, N. & Maio, M. (2014) Peptide-based vaccines for cancer therapy. *Hum. Vaccin. Immunother.*, **10**, 3175-3178.

Ricci, V., Fabozzi, T., Bareschino, M.A., Barletta, E., Germano, D., Paciolla, I., Tinessa, V. & Grimaldi, A.M. (2022) Pancreatic cancer: beyond BRCA mutations. *J. Pers. Med.*, **12**, 2076.

Salmaninejad, A., Zamani, M.R., Pourvahedi, M., Golchehre, Z., Hosseini Bereshneh, A. & Rezaei, N. (2016) Cancer/testis antigens: expression, regulation, tumor invasion, and use in immunotherapy of cancers. *Immunol. Invest.*, **45**, 619-640.

Sato, Y. (2013) The vasohibin family: a novel family for angiogenesis regulation. *J. Biochem.*, **153**, 5-11.

Saxena, M., van der Burg, S.H., Melief, C.J.M. & Bhardwaj, N. (2021) Therapeutic cancer vaccines. *Nat. Rev. Cancer*, **21**, 360-378.

Shibuya, T., Watanabe, K., Yamashita, H., Shimizu, K., Miyashita, H., Abe, M., Moriya, T., Ohta, H., Sonoda, H., Shimosegawa, T., Tabayashi, K. & Sato, Y. (2006) Isolation and characterization of vasohibin-2 as a homologue of VEGF-inducible endothelium-derived angiogenesis inhibitor vasohibin. *Arterioscler. Thromb. Vasc. Biol.*, **26**, 1051-1057.

Suzuki, Y., Kitahara, S., Suematsu, T., Oshima, M. & Sato, Y.

(2017) Requisite role of vasohibin-2 in spontaneous gastric cancer formation and accumulation of cancer-associated fibroblasts. *Cancer Sci.*, **108**, 2342-2351.

Suzuki, Y., Kobayashi, M., Miyashita, H., Ohta, H., Sonoda, H. & Sato, Y. (2010) Isolation of a small vasohibin-binding protein (SVBP) and its role in vasohibin secretion. *J. Cell Sci.*, **123**, 3094-3101.

Takahashi, Y., Koyanagi, T., Suzuki, Y., Saga, Y., Kanomata, N., Moriya, T., Suzuki, M. & Sato, Y. (2012) Vasohibin-2 expressed in human serous ovarian adenocarcinoma accelerates tumor growth by promoting angiogenesis. *Mol. Cancer Res.*, **10**, 1135-1146.

Tu, M., Li, Z., Liu, X., Lv, N., Xi, C., Lu, Z., Wei, J., Song, G., Chen, J., Guo, F., Jiang, K., Wang, S., Gao, W. & Miao, Y. (2017) Vasohibin 2 promotes epithelial-mesenchymal transition in human breast cancer via activation of transforming growth factor beta 1 and hypoxia dependent repression of GATA-binding factor 3. *Cancer Lett.*, **388**, 187-197.

Watanabe, K., Hasegawa, Y., Yamashita, H., Shimizu, K., Ding, Y., Abe, M., Ohta, H., Imagawa, K., Hojo, K., Maki, H., Sonoda, H. & Sato, Y. (2004) Vasohibin as an endothelium-derived negative feedback regulator of angiogenesis. *J. Clin. Invest.*, **114**, 898-907.

Xue, X., Gao, W., Sun, B., Xu, Y., Han, B., Wang, F., Zhang, Y., Sun, J., Wei, J., Lu, Z., Zhu, Y., Sato, Y., Sekido, Y., Miao, Y. & Kondo, Y. (2013) Vasohibin 2 is transcriptionally activated and promotes angiogenesis in hepatocellular carcinoma. *Oncogene*, **32**, 1724-1734.

Xue, X., Zhang, Y., Zhi, Q., Tu, M., Xu, Y., Sun, J., Wei, J., Lu, Z., Miao, Y. & Gao, W. (2014) MiR200-upregulated Vasohibin 2 promotes the malignant transformation of tumors by inducing epithelial-mesenchymal transition in hepatocellular carcinoma. *Cell Commun. Signal.*, **12**, 62.

Yoshida, S., Nakagami, H., Hayashi, H., Ikeda, Y., Sun, J., Tenma, A., Tomioka, H., Kawano, T., Shimamura, M., Morishita, R. & Rakugi, H. (2020) The CD153 vaccine is a senotherapeutic option for preventing the accumulation of senescent T cells in mice. *Nat. Commun.*, **11**, 2482.

Zhang, Y., Xue, X., Zhao, X., Qin, L., Shen, Y., Dou, H., Sun, J., Wang, T. & Yang, D.Q. (2018) Vasohibin 2 promotes malignant behaviors of pancreatic cancer cells by inducing epithelial-mesenchymal transition via Hedgehog signaling pathway. *Cancer Med.*, **7**, 5567-5576.

## Supplementary Files

Please find supplementary file(s);
https://doi.org/10.1620/tjem.2023.J076